Development 134, 1133-1140 (2007) doi:10.1242/dev.000265

Hippocampus-like corticoneurogenesis induced by two isoforms of the BTB-zinc finger gene *Zbtb20* in mice

Jakob V. Nielsen, Flemming H. Nielsen, Rola Ismail, Jens Noraberg and Niels A. Jensen*

Hippocampus-associated genes that orchestrate the formation of the compact stratum pyramidale are largely unknown. The BTB (broad complex, tramtrack, bric-a-brac)-zinc finger gene *Zbtb20* (also known as *HOF*, *Znf288*, *Zfp288*) encodes two protein isoforms, designated Zbtb20^{S} and Zbtb20^{L}, which are expressed in newborn pyramidal neurons of the presumptive hippocampus in mice. Here, we have generated transgenic mice with ectopic expression of Zbtb20^{S} and Zbtb20^{L} in immature pyramidal neurons differentiated from multipotent non-hippocampal precursors. The subiculum and posterior retrosplenial areas in these mice were transformed into a three-layered hippocampus-like cortex with a compact homogenous pyramidal cell layer. Severe malformations of lamination occur in neocortical areas, which coincide with a deficiency in expression of cortical lamination markers. The alterations in cortical cytoarchitecture result in behavioral abnormalities suggestive of a deficient processing of visual and spatial memory cues in the cerebral cortex of adult Zbtb20 transgenic mice. Overall, our in vivo data suggest that Zbtb20 functions as a molecular switch for a pathway that induces invariant pyramidal neuron morphogenesis and suppression of cell fate transitions in newborn neurons.

KEY WORDS: Zbtb20, HOF, Zfp288, Znf288, BTB, Zinc finger, Cerebral cortex, Hippocampus, Development, Pyramidal neuron, Neurogenesis, Lamination, Migration

INTRODUCTION

The hippocampal formation is composed of neurons that process information essential for cognitive functions such as memory and learning. Six cortical areas constitute the hippocampal formation: hippocampus (or Ammon's horn), dentate gyrus (DG), subiculum, presubiculum, parasubiculum and entorhinal cortex (Johnston and Amaral, 1998). Morphologically homogenous neurons constitute the compact granule cell layer of the DG and the CA1 and CA3 pyramidal cell layer (or stratum pyramidale) of the hippocampus. The subiculum comprises three distinct subtypes of large pyramidal neurons that form the less-compact pyramidal cell layer of this area (Ishizuka, 2001), whereas other areas of the hippocampal formation, the transitional retrosplenial cortex and the neocortex, harbor several subsets of pyramidal neurons organized in deep and upper layers (Monuki and Walsh, 2001). Neurogenesis of projection neurons in the dorsal telencephalon follows a common path with area fate determination, activity-dependent refinement and an inside-out developmental sequence, where first-born neurons reside in deep layers of the cortical plate (CP) and later-born neurons prevail in outer layers (Sur and Rubenstein, 2005). Cortical pyramidal neurons are generated by asymmetric divisions of radial glia and progenitors within the ventricular zone (VZ) and subventricular zone (SVZ) of the dorsal telencephalon, and migrate to the CP along radially oriented processes of radial glia (Rakic, 2006). Generation of projection neurons from cortical progenitors appears to be governed by both cell-intrinsic and environmental cues (Fishell, 1995; McConnell and Kaznowski, 1991; Mizutani and Gaiano, 2006; Qian et al., 1997). Cortical stem cells and progenitors harbor a cell-intrinsic mechanism by which they can generate preplate-like cells, deep and outer layer-like neurons and macroglia in a 'normal' developmental sequence in vitro (Shen et al., 2006).

There are two notable developmental specializations to neurogenesis of the hippocampal stratum pyramidale. First, immature pyramidal neurons in the hippocampus migrate more slowly to the CP compared with the neocortical pyramidal neurons (Altman and Bayer, 1990; Nakahira and Yuasa, 2005). Second, whereas lamination of most areas of the cerebral cortex results from a process we refer to as variant corticoneurogenesis, lamination of the hippocampus results from invariant corticoneurogenesis. The former developmental process gives rise to the great diversity of pyramidal neurons in the neocortical areas. The latter generates the two morphologically homogenous CA1 and CA3 neuronal populations that constitute the stratum pyramidale of the hippocampus. Defects in lamination of the hippocampus are common in human congenital malformations of cortical lamination (Montenegro et al., 2006; Tanaka et al., 2006) and in mice lacking the microtubule-associated proteins Doublecortin and Doublecortin-like (Corbo et al., 2002; Tanaka et al., 2006).

Assuming that progenitors and newborn neurons are exposed to cell-intrinsic and external changes in cues that trigger fate transitions, how is the area-specific invariant morphogenesis of pyramidal neurons in Ammon's horn accomplished? A number of genes have been shown to be important for various aspects of neurogenesis in the hippocampus including proliferation and specification of progenitors (Galceran et al., 2000; Lee et al., 2000; Machon et al., 2003; Miyata et al., 1999; Ohkubo et al., 2004; Tole et al., 2000; Zhao et al., 1999). The mammalian BTB-zinc finger gene *Zbtb20* (also known as *HOF*, *Znf288*, *Zfp288*), hereon referred to as *Zbtb20*, is expressed during the critical period of neurogenesis of pyramidal neurons in areas CA3 and CA1 of the mouse hippocampus (Mitchelmore et al., 2002). Here we show that Zbtb20 induces hippocampus-like corticoneurogenesis in the mouse brain following ectopic expression of the gene in non-hippocampal

Molecular Neurobiology Laboratory, Medical Biotechnology Center, University of Southern Denmark, J. B. Winslowsvej 25, DK-5000 Odense C, Denmark.

*Author for correspondence (e-mail: naajensen@health.sdu.dk)

Accepted 5 January 2007

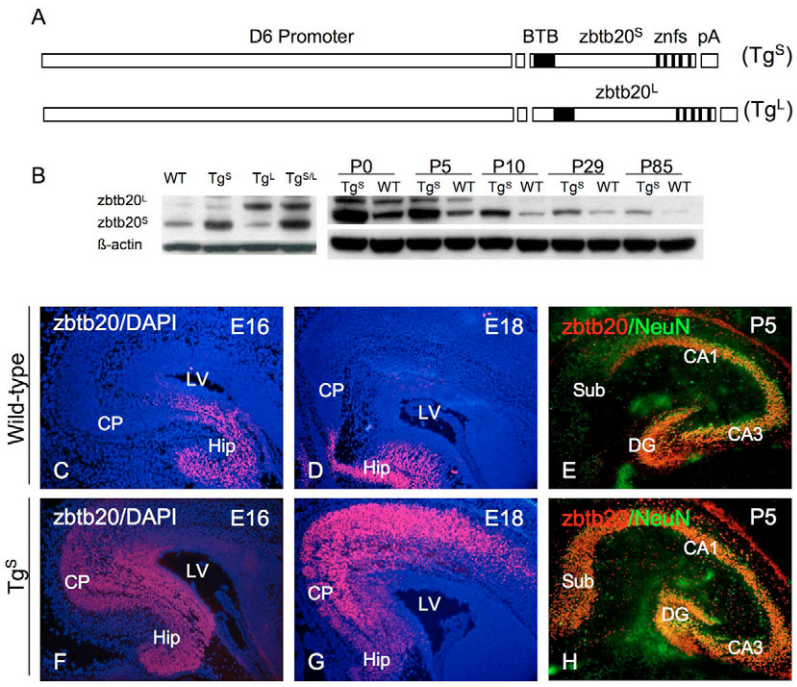

Fig. 1. Zbtb20 misexpression in dorsal telencephalon of transgenic mice. (**A**) Schematic illustration of the Zbtb20^{S} and Zbtb20^{L} recombinant constructs used for pronuclear microinjection. (**B**) Western blot analysis of Zbtb20^{S} and Zbtb20^{L} expression in the hippocampal formation of wild-type mice and mice harboring D6/Zbtb20^{S} (Tg^{S}), D6/Zbtb20^{L} (Tg^{L}) and D6/Zbtb20^{S}//D6/Zbtb20^{L} (Tg$^{S/L}$) transgenes (left). Western blot analysis of postnatal Zbtb20 expression in the hippocampal formation of Tg^{S} and wild-type littermates (right). (**C**,**D**,**F**,**G**) Indirect immunofluorescent detection in wild-type and Tg^{S} E16 and E18 coronal hemisections of Zbtb20 protein, counterstained with DAPI. (**E**,**H**) Horizontal sections of P5 wild-type and Tg^{S} hippocampal formations showing co-expression of Zbtb20 (red) and NeuN (green) by indirect immunofluorescence. CA1 and CA3 indicate hippocampus; CP, cortical plate; DG, dentate gyrus; Hip, presumptive hippocampus; LV, lateral ventricle; Sub, subiculum; WT, wild type.

immature pyramidal neurons. We furthermore find that Zbtb20 delays the radial migration of immature cortical neurons and orchestrates the formation of a CA-like pyramidal cell layer in the subiculum and posterior retrosplenial cortex.

MATERIALS AND METHODS

Transgenic mice and in utero electroporation

The D6 promoter-enhancer (Machon et al., 2002) was inserted into Zbtb20^{S} and Zbtb20^{L} expression plasmids. For microinjection, the D6/Zbtb20^{S} and D6/Zbtb20^{L} transgenes were excised from the plasmid vector, gel-purified and microinjected, at a concentration of 6 ng/μL, into the pronucleus of fertilized mouse eggs as previously described (Jensen et al., 1993). A total of five transgenic mouse lines (two D6/Zbtb20^{S} and three D6/Zbtb20^{L}) with ectopic cortical Zbtb20 expression were generated. All five lines displayed similar structural alterations in cortical lamination ruling out insertional mutagenesis as a cause of the phenotype. Accordingly, we selected two representative Zbtb20 transgenic lines (one D6/Zbtb20^{S} and one D6/Zbtb20^{L}) for the studies described in this report. Transgenic mice were identified by PCR genotyping of genomic DNA purified from tail biopsies, using the Wizard genomic DNA purification kit (Promega). The primers used for the PCR analysis were: 5′-GAGAGAGGACTCGCATTTC-GACTTG-3′ and 5′-GATGCGAACCGTCACGTCACAGAAG-3′, which produce a 354 bp PCR product using genomic DNA from D6/Zbtb20^{S} mice as template, and a 573 bp product using DNA from D6/Zbtb20^{L} mice as template.

Transfection of cells in vivo by in utero electroporation was performed as previously described (Nakahira and Yuasa, 2005; Tabata and Nakajima, 2001). Briefly, multiparous mice at 15 days of gestation were deeply anesthetized, and the uterine horns were exposed. Approximately 1 μL of pCIG2-EGFP plasmid (Hand et al., 2005), at a concentration of 4 μg/μL with 0.01% Fast Green (Sigma), was injected through the uterus into the lateral ventricles of embryos. Eight 50-millisecond electric pulses of 40 V were delivered in intervals of 80 milliseconds, directing the DNA towards the medial-dorsal telencephalon. The voltage pulse was discharged using a pair of disc-electrodes placed on either side of the head of each embryo through the uterus. The uterus was placed back in the abdominal cavity to allow embryonic development to continue to term. Brains from neonatal (P0) and P14 mice were dissected out and fixed overnight in 4% paraformaldehyde (PFA), embedded in 5% agar in phosphate-buffered saline (PBS) and subsequently sectioned at 100 μm using a vibratome (Leica VT1000S). The sections were counterstained with DAPI, and enhanced green fluorescent protein (EGFP) fluorescent (EGFP^{+}) cells were visualized and photographed. For cell counting, four subregions in the P0 cerebral cortex [VZ/SVZ, intermediate zone (IZ), deep and superficial half of the CP] were identified based on cell density, as visualized with DAPI. The total number of EGFP^{+} cells in each region was counted in two adjacent coronal sections at mid-posterior axial levels from three Zbtb20^{S} transgenic mice (2200 cells in total) and three control mice (3000 cells in total). All animal protocols were approved by the Danish Ministry of Justice Animal Care and Use Committee.

Golgi staining

Modified Golgi-Cox impregnation of neurons was performed using specifications described in the FD Rapid GolgiStain Kit (FD Neurotechnologies). In brief, 2-month-old mouse brains were immersed in impregnation solution for 2 weeks, transferred to ‘Solution C’ for 2 days, embedded in 5% agar in PBS and cut at 100 μm on the microtome. Sections were mounted on superfrost plus slides (Menzel-Gläser) and dried for 2 weeks prior to staining with silver nitrate solution ‘Solution D and E’. The sections were dehydrated and mounted with Depex.

Immunohistochemistry

In some cases, mice were given an intraperitoneal injection of 0.1 mg of bromodeoxyuridine (BrdU)/g body weight (diluted in physiological saline) before they were sacrificed. The brains were removed and immediately frozen in liquid nitrogen. Cryostat-cut brain sections (20 μm) were collected on superfrost plus slides, fixed with methanol for 5 minutes and incubated for 1 hour at 37°C or overnight at 4°C, in the presence of a primary antibody that was diluted in PBS with 0.1% Triton X-100. The following primary antibodies were used at 1:100 dilution unless otherwise stated: rabbit Zbtb20 (Mitchelmore et al., 2002); mouse NeuN (Chemicon); mouse reelin (Abcam); goat Brn-1 and goat Brn-2 (Santa Cruz); rabbit Oct-6, diluted 1:500 (Sock et al., 1996). For staining with sheep BrdU antisera, diluted 1:200 (Research Diagnostics), the fixed sections were first treated for 30 seconds each with 2 M HCl and 0.1 M borate. After rinsing in PBS, sections were incubated for 1 hour at 37°C in secondary antibody diluted in PBS with 0.1% Triton X-100, washed in PBS and mounted with Vectashield mounting medium with DAPI (Vector Laboratories). The following secondary antibodies were used at 1:100 dilution: TRITC-conjugated swine anti-rabbit;

FITC-conjugated goat anti-mouse; FITC-conjugated rabbit anti-mouse; FITC-conjugated rabbit anti-goat (DAKO); and FITC-conjugated donkey anti-sheep (Research Diagnostics Inc.). ER81 immunohistochemistry was carried out on 20 μm PFA-fixed cryosections, which were first incubated for 2 hours in PBS containing 10% normal goat serum and 0.1% Triton X-100. Sections were then incubated for 48 hours at 4°C with the primary rabbit ER81 antibody (Arber et al., 2000), diluted 1:200 in PBS containing 0.1% Triton X-100. After rinsing in PBS, sections were incubated for 1 hour at 37°C in biotinylated goat anti-rabbit antibody (DAKO), in PBS containing 0.1% Triton X-100. Sections were then rinsed in PBS and incubated in Vectastain Elite ABC Reagent using diaminobenzidine tetrahydrochloride (DAB) as the substrate, according to the manufacturer's instructions (Vector Laboratories).

Western blot

Dissected hippocampi were homogenized on ice in 100 μL of RIPA buffer containing 450 mM NaCl, 1 mM dithiothreitol, and 0.2% v/v protein inhibitor mixture (Sigma). After 30 minutes on ice, the extracts were spun at 14,000×***g*** for 10 minutes at 4°C, and the supernatants were recovered. The protein concentrations were measured (Bio-Rad), and 20 μg of each extract was loaded onto a 4-12% NuPAGE Bis-Tris gel (Novex). Western blots were analyzed using the ECL Advance Western Blotting Detection Kit (Amersham). The primary rabbit Zbtb20 and mouse β-actin (Sigma) antibodies were used at 1:5000 dilutions.

Behavioral tests

A total of 13 Zbtb20^{S} transgenic and 11 wild-type adult female littermate mice were used in the behavioral test. The two groups of mice were housed three to five together in standard cages with ad libitum access to food and water. All animals were maintained on a 12-hour light-dark cycle. The visual cliff test was performed between 10.00 h and 14.00 h, and the circular platform maze test was performed between 18.00 h and 23.30 h.

The visual cliff test apparatus was prepared according to specifications described elsewhere (Fox, 1965). It consists of an elevated horizontal plane (safe side) connected to a 60 cm vertical drop followed by a second horizontal plane (deep side). Both horizontal planes were covered with 2 cm^2 black and white checkerboard pattern paper to accentuate the vertical drop-off. A sheet of clear Plexiglas was placed across the top horizontal plane, extending across the cliff so that there was no actual drop-off, just the visual appearance of a cliff. The edge of the cliff harbors a ridge of aluminium, 40 mm high and 25 mm wide. Each mouse was placed on the aluminium block at the start of ten consecutive trials, and allowed to step down to one of the sides (safe or deep). The choice of side was recorded.

The circular platform maze was carried out as previously described (Pompl et al., 1999) with some modifications. Briefly, the behavioral testing consisted of 17 trials, with one trial per day. During the first 10 days of the trial (the learning period) the location of the escape box was maintained in the same position. In the reverse learning period, which lasted for a total of 7 days, the escape box was moved to a new position 180° from its previous location. Mice were introduced into the maze at three different orientations relative to the escape hole (90°, 180° or 270°). Each mouse was allowed a maximum of 300 seconds per trial. The total numbers of errors (nose pokes into non-escape holes) and latency to enter the escape hole were recorded. During the reverse learning period, the mice were introduced into the maze at orientations of 90° or 270° to the escape hole. The number of nose pokes into the learning period escape hole was recorded as 'probes'.

Statistics

The percentage of EGFP^{+} cells in each of the four cortical subregions was compared between control and Zbtb20^{S} transgenic mice using Student's *t* test. The preference for stepping down to the safe or deep side of the visual cliff was analyzed using paired Student's *t* test. The number of steps to the safe side was analyzed using Student's *t* test. Circular platform maze data including latencies and errors to find the escape hole during the learning period (days 1 to 10) and the reverse learning period (days 11-17) were analyzed using repeated measures (RM) analysis of variance (ANOVA). Paired Student's *t* test was used to compare the number of errors and escape latencies between days 10 and 11. Student's *t* test was used to analyze differences in latencies (on the same day) and errors (at day 17) between the two groups of mice. In addition, Student's *t* test was used to compare the number of probes to the learning period escape hole at day 11 with the number of probes to each of the remaining 15 holes. Whenever the data were not normally distributed, the median values were compared using the Mann–Whitney rank sum test. A *P*-value of less than or equal to 0.05 was considered to be significant. All data are depicted as means±s.e.m. All statistics were done using SigmaStat (SPSS).

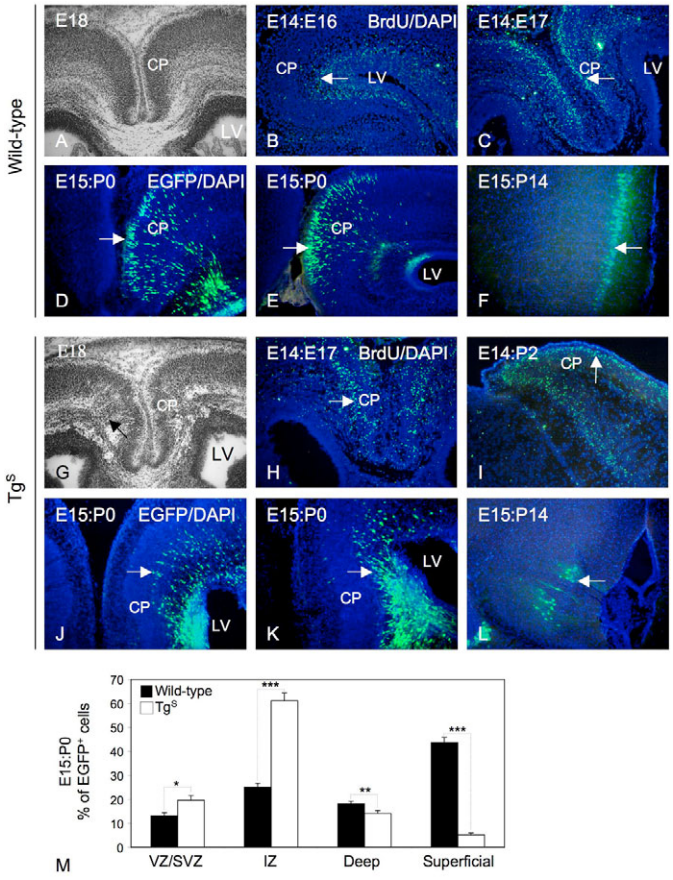

Fig. 2. Delayed radial migration of immature projection neurons in Zbtb20 transgenic mice. (**A**,**G**) Nissl-stained wild-type and Zbtb20 transgenic E18 coronal sections of medial-dorsal telencephalon. Compared with wild type (A), Zbtb20 transgenic embryos harbor streams of radial migrating cells in the intermediate zone (arrow in G). (**B-F**,**H-L**) Cell birth date and cortical migration analyses by indirect immunofluorescent detection of BrdU-labeled cells (arrows in B,C,H,I) and by fluorescent visualization of EGFP-labeled neurons in CP (arrows in D-F,J-L) at late P0 (D,E,J,K) and P14 (F,L) following in vivo transfection with a pCIG2-EGFP expression vector at E15, in coronal sections counterstained with DAPI. (**M**) Distribution of EGFP-labeled cells in P0 brains transfected with pCIG2-EGFP at E15.The data are presented as means±s.e.m. *, P=0.021, **, P=0.029, ***, $P\leqslant$0.001. Deep, deep half of CP; Superficial, superficial half of CP.

RESULTS

To reveal a role for Zbtb20 in cortical neurogenesis, we studied the consequences of ectopic expression of Zbtb20^{S} and Zbtb20^{L} both separately and together during cortical projection neuron development in mice (Fig. 1A,B). In wild-type brains, the two isoforms of Zbtb20 are expressed in developing projection neurons of the prospective hippocampus and DG with a sharp decline in expression at the subicular border (Fig. 1C-E). Zbtb20 is present in

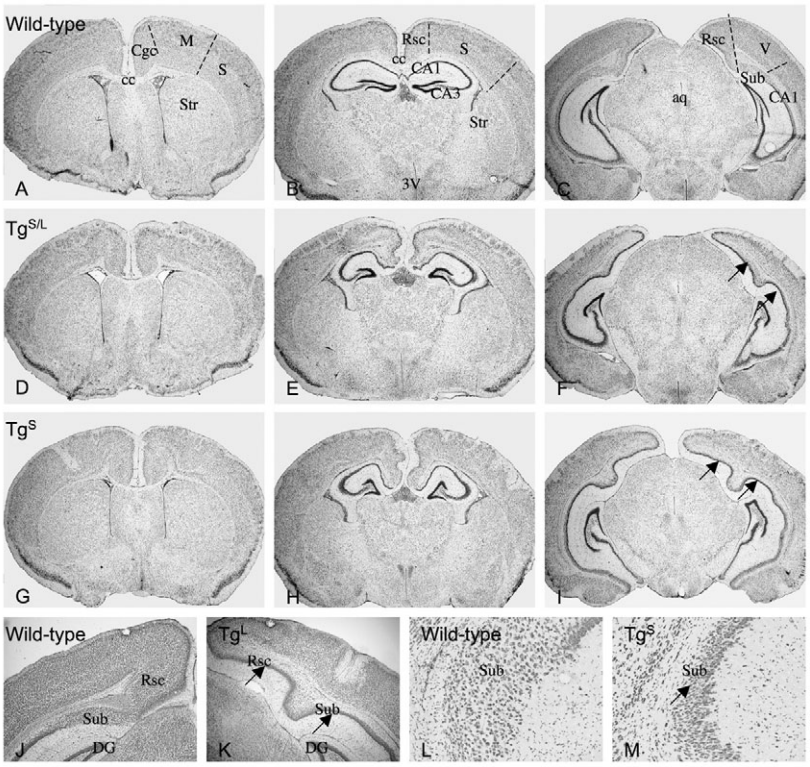

Fig. 3. Cortical lamination defects and hippocampus-like cytoarchitectonic transformations. (**A-K**) Nissl-stained adult wild-type, $Tg^{S/L}$, Tg^{S} and Tg^{L} coronal forebrain sections at rostral (A,D,G), mid (B,E,H) and caudal axial levels, in low (C,F,I) and high (J,K) magnification views. Note the compact hippocampus-like pyramidal cell layer in subicular (Sub) and retrosplenial areas (Rsc) in Tg^{S}, $Tg^{S/L}$ and Tg^{L} brains (arrows in F,I,K). (**L**,**M**) Nissl-stained adult wild-type and Tg^{S} transgenic horizontal sections showing that the subicular pyramidal cell layer in the Zbtb20 transgenic mice is transformed into a compact hippocampus-like pyramidal cell layer in Tg^{S} (arrow in M). aq, aqueduct of Sylvius; cc, corpus callosum; Cgc, cingulate cortex; DG, dentate gyrus; M, motor cortex; S, somatosensory cortex; Str, striatum (caudate putamen); 3V, third ventricle; V, visual cortex.

cells located in upper SVZ, IZ and CP of the hippocampal primordium (Fig. 1C,D). In D6/Zbtb20 (Zbtb20) transgenic mice, this pattern of Zbtb20 expression is copied to newborn and radial migrating projection neurons in presumptive subicular, transitional and neocortical areas (Fig. 1F-H). Zbtb20 colocalizes with the general neuronal marker NeuN in nuclei of projection neurons in the hippocampus of wild-type brains (Fig. 1E) and in areas with ectopic expression of Zbtb20 in transgenic brains (e.g. subiculum in Fig. 1H).

Compared with the wild-type embryos (Fig. 2A), the medial dorsal telencephalon of Zbtb20 transgenic embryos harbors streams of migrating cells in the IZ, which is suggestive of a deficiency or a delay in radial migration of immature cortical neurons (Fig. 2G). We next used bromodeoxyuridine (BrdU) birth-dating analyses to determine the migration of cortical projection neurons in wild-type brains and in brains of Zbtb20 transgenic littermates. The pattern of BrdU-labeled cells was compared in medial regions of the dorsal-caudal telencephalon. Wild-type neurons labeled at E14 and analyzed at E16 revealed numerous cells in the upper SVZ and IZ (Fig. 2B), whereas at E17 these cells are mainly present in outer layers of the CP (Fig. 2C). This migration pattern is consistent with the inside-out gradient of cortical projection neuron histogenesis. At E17, a majority of neurons labeled with BrdU at E14 still reside below the CP in Zbtb20 transgenic brains (Fig. 2H), whereas at postnatal day 2 (P2) they have settled in outer layers of the CP (Fig. 2I). A delayed radial migration of neurons born in the VZ of the dorsal telencephalon of Zbtb20 transgenic mice was further documented by transfecting radial glia in transgenic and normal littermate embryos with a mammalian expression vector encoding EGFP. More than 40% of neurons derived from radial glia tagged with the EGFP reporter at E15 have settled in the outer half of the CP in wild-type P0 brains, with approximately 25% of cells in the IZ (Fig. 2D,E,M) consistent with their outer layer fate. An outer layer fate of these cells was further confirmed in E15 to P14 animals (Fig. 2F). In Zbtb20 transgenic P0 brains, only about 5% of neurons born after E15 have settled in the outer half of the CP, with most labeled cells (about 60%) in the IZ (Fig. 2J,K,M), whereas at P14 these cells have settled in outer layers of the neocortex (Fig. 2L). Thus, although neurons appear to settle in the CP in an inside-out developmental sequence, there appears to be a transient accumulation of radial migrating cells in the IZ of Zbtb20 transgenic mice.

Similar malformations of cortical development, which generally appear to be most pronounced at medial-posterior levels along the anterior-posterior axis, are observed in adult $Zbtb20^{S}$, $Zbtb20^{L}$ and $Zbtb20^{S/L}$ transgenic mice (Fig. 3A-M and data not shown). Although present at anterior axial positions (Fig. 3A,D,G), the corpus callosum is lacking at more posterior levels (Fig. 3B,E,H). At medial-posterior positions, the subicular and retrosplenial areas are transformed into a three-layered archicortex composed of a compact hippocampus-like pyramidal cell layer and a markedly expanded apical dendrite layer (Fig. 3C,F,I,J,K). The compact CA-like laminar transformation of the subiculum was confirmed in horizontal brain sections (Fig. 3L,M). The transformed retrosplenial area of Zbtb20 transgenic mice comprises a single stratum pyramidal-like cell layer composed of large homogeneous-appearing neurons with a marginal zone projecting apical dendrites (Fig. 4). The transformed neurons are typical pyramidal-like with basal and apical dendrites covered with spines, and they show a morphologic resemblance to CA1 pyramidal cells (Fig. 4F,G).

As developmental transformations of the Zbtb20 transgenic cortex are most pronounced at posterior axial levels, we performed molecular marker analyses on subicular, posterior retrosplenial and visual areas. The transcription factor Oct-6 (Pou3f1; also known as Scip and Tst1) is a marker of CA1 and layer V pyramidal neurons in adult rodent brains (Fig. 5A,B) (Frantz et al., 1994). In Zbtb20 transgenic brains, there is a robust Oct-6 immunostaining of cells in subicular and medial retrosplenial areas, which is similar in intensity to that of cells in the CA1 area of the hippocampus (Fig. 5G,H), but different from the scattered staining of cells in wild-type subicular and medial

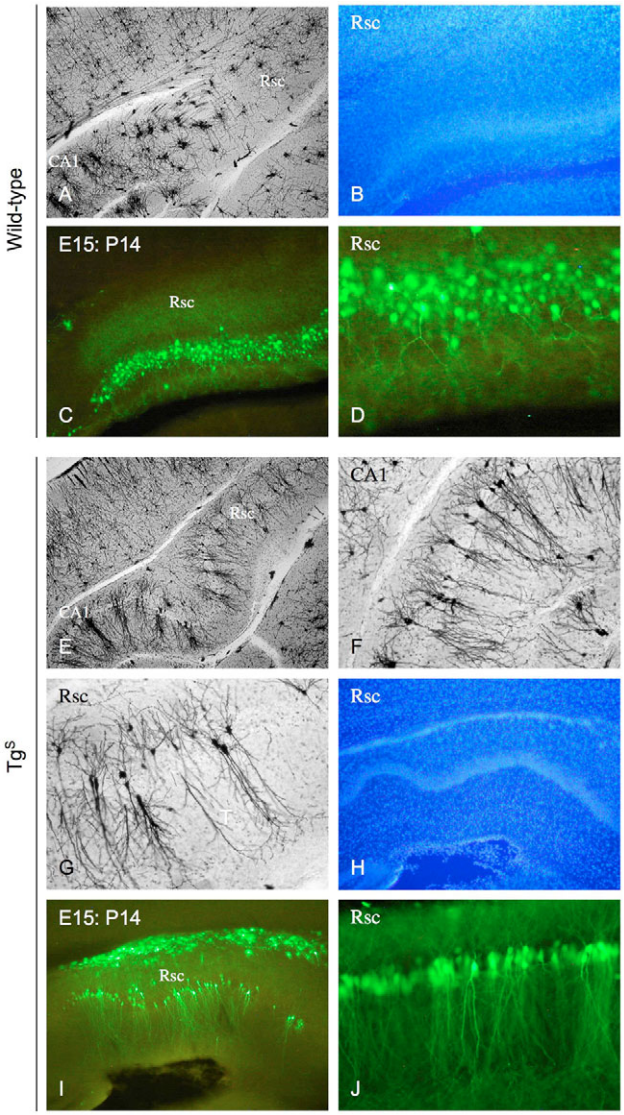

Fig. 4. The transformed retrosplenial cortex is composed of large hippocampus-like pyramidal neurons. (**A**,**E-G**) Golgi impregnation of wild-type (A) and Tg^S transgenic (E-G) posterior Rsc revealing a CA1-like morphology of pyramidal neurons. (**B-D**,**H-J**) Alterations in pyramidal neuron morphology in Tg^S transgenic (H-J) posterior Rsc compared with wild type (B-D) shown by fluorescent visualization of EGFP-labeled outer layer neurons at P14, following in vivo transfection with a pCIG2-EGFP expression vector at E15, in coronal sections counterstained with DAPI (B,H). Note that Rsc pyramidal neurons born after E15 in Tg^S transgenic brains are large cells that settle in a compact pyramidal cell layer (J), whereas these neurons are small outer-layer pyramids in wild-type brains (D).

retrosplenial areas (Fig. 5A,B). The ETS family transcription factor ER81 (Etv1 – Mouse Genome Informatics) is expressed in subsets of subicular and layer V pyramidal neurons in various cortical areas including the retrosplenial cortex (Fig. 5C) (Yoneshima et al., 2006). In contrast to wild-type brains, ER81-positive cells were not revealed in subicular and retrosplenial areas of Zbtb20 transgenic brains (Fig. 5I), further supporting the notion of a CA-like transformation of these regions. Expression of Brn-1 and Brn-2 (Pou3f3 and Pou3f2, respectively – Mouse Genome Informatics), markers of superficial cortical layers and SVZ of the neocortex at P0 (McEvilly et al., 2002), was detected in upper CP and SVZ by immunohistochemistry of wild-type brains (Fig. 5D,E), but was not revealed in visual (dorsal) and posterior retrosplenial (medial) areas of Zbtb20 transgenic brains (Fig. 5J,K). In lateral areas of the Zbtb20 transgenic visual cortex, Brn-1 and Brn-2 immunoreactive cells formed cortical nodules in superficial layers that are separated from deep layers by a cell-sparse transition zone (Fig. 5M-P). Reelin is a glycoprotein secreted from a population of early appearing cortical neurons termed Cajal-Retzius (CR) cells that settle in the marginal zone (D'Arcangelo et al., 1997). The protein appears to guide placement of migrating projection neurons in the CP. Reelin-positive CR cells were found in the marginal zone of the cerebral cortex in both normal mice (Fig. 5F) and Zbtb20 transgenic littermates (Fig. 5L). Thus, there appears to be a deficiency in subsets of deep and outer layer pyramidal neurons in Zbtb20 transgenic brains.

We next tested whether or not malformations in Zbtb20 transgenic brains are associated with behavioral abnormalities. Two groups of age-matched adult $Zbtb20^S$ transgenic and wild-type littermates were challenged by the visual cliff test, which measures the animal's ability to see the drop-off at the edge of a horizontal surface and serves as a gross measure of visual capability (Fox, 1965). Consistent with a deficiency in processing visual cues (Fig. 6A), Zbtb20 transgenic mice stepped down to both the safe and deep sides at roughly equal frequencies (P=0.157), whereas the wild-type littermate mice showed a strong preference for the safe side (P<0.001). The two groups of mice were furthermore tested in the circular platform or Barnes maze, which measures spatial navigation memory (Pompl et al., 1999). In the 10-day learning period, both wild-type and Zbtb20 transgenic mice showed a statistically significant improvement in performance (Fig. 6B and see Table S1 in the supplementary material) that correlated with a significant reduction in errors prior to locating the escape box (Fig. 6C). However, wild-type mice appeared to use spatial cues to move directly to the escape hole, whereas Zbtb20 transgenic mice explored the periphery of the platform to locate the same hole. In the reverse learning period (starting at day 11), the escape box was moved to a new location 180° relative to the old position. At the first trial day of this phase, the wild-type mice, but not the transgenic mice, showed a statistically significant increase in latency and number of errors (P=0.007 and P=0.002, respectively) compared with the last trial day of the learning period (Fig. 6B,C). To reveal whether or not the two groups of mice have recollection of the location of the learning period escape hole, the number of visits to this hole (probes) was compared with the number of visits to each of the remaining 15 holes on the first day of the reverse learning period. The wild-type mice showed a preference for the old escape hole that was not observed in the transgenic group (Fig. 6D and see Table S2 in the supplementary material). Thus, whereas wild-type mice appear to remember the location of the escape hole from the learning phase, Zbtb20 transgenic mice apparently have no recollection of this hole. Moreover, there was an apparent improvement in the wild-type group to locate the escape hole that correlated with a statistically significant decline in both escape latency (P<0.001) and number of errors (P<0.001). A similar statistically significant effect was not revealed in the Zbtb20 transgenic group (Fig. 6B,C). For example at trial day 17, the wild-type mice were significantly faster at locating the escape hole (P=0.003), and made significantly fewer errors than the Zbtb20 transgenic mice (P<0.001).

DISCUSSION

In the present study, ectopic expression of $Zbtb20^S$ and $Zbtb20^L$ isoforms has made it possible to examine a novel function for this BTB-zinc finger factor in regulation of invariant cortical

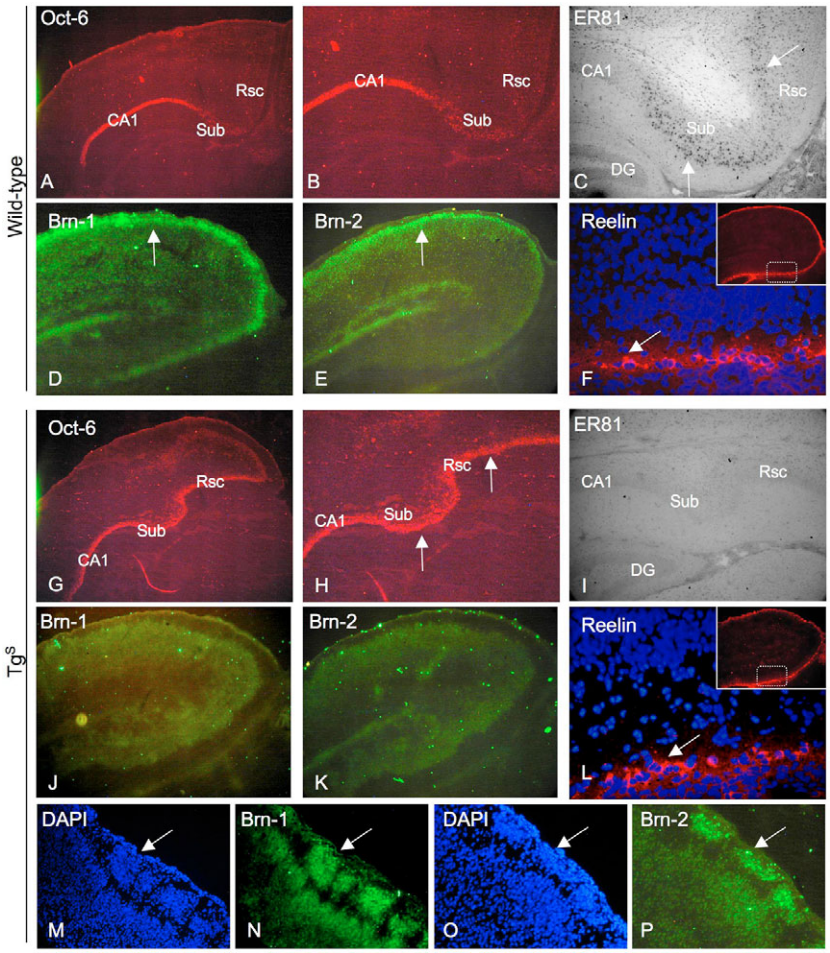

Fig. 5. Altered pattern of molecular marker expression in Zbtb20^S transgenic cortex. (**A**,**G**) Low-magnification views of indirect immunofluorescent detection of Oct-6-labeled cells in coronal sections of P14 wild-type (A) and Zbtb20 transgenic (G) posterior cerebral cortex. (**B**,**H**) Higher-magnification views of A and G with focus on CA1, Sub and Rsc. (**C**,**I**) Immunohistochemical detection of ER81-labeled cells in coronal sections of P14 wild-type (C) and Zbtb20 transgenic (I) CA1, Sub and posterior Rsc. (**D**,**E**,**J**,**K**) Indirect immunofluorescent detection of Brn-1- and Brn-2-labeled cells in coronal sections of P0 wild-type (arrows in D and E) and Zbtb20 transgenic (J,K) posterior cerebral cortex. (**F**,**L**) High-magnification views of indirect immunofluorescent detection of reelin (arrows) in retrosplenial cortex of coronal hemisections of P0 wild-type (F) and Zbtb20 transgenic (L) brains. Insets (F,L), low-magnification views of indirect immunofluorescent detection of reelin in posterior cerebral cortex. (**M-P**) Indirect immunofluorescent detection of Brn-1 and Brn-2 expression in sub-pial nodules (arrows in N and P) of lateral areas of Zbtb20 transgenic visual cortex, counterstained with DAPI (M,O).

neurogenesis in mice. The hippocampus-like cytoarchitectonic transformations of subicular and posterior retrosplenial areas are characterized by (1) a delayed migration of immature neurons to the CP and (2) the generation of an Ammon's horn-like pyramidal cell layer. A similar phenotype was revealed in Zbtb20^S, Zbtb20^L and Zbtb20$^{S/L}$ transgenic mice, suggesting an overlap in function of the two Zbtb20 isoforms.

In wild-type brains, Zbtb20 appears not to be expressed in nuclei of radial glia or in dividing cortical progenitors (Mitchelmore et al., 2002). The gene is turned on in newborn immature pyramidal neurons in upper layers of the SVZ in the presumptive hippocampus and is downregulated in these cells during the second postnatal week. Ectopic Zbtb20 expression in newborn neurons was shown to occur in medial areas of the dorsal telencephalon of Zbtb20 transgenic mice. The extent of lamination of the neocortex was more variable compared with the transitional posterior retrosplenial cortex, with some areas harboring only a thin sheath of cells and a markedly expanded layer I (e.g. Fig. 3G,H,K). Our preliminary analyses of ectopic Zbtb20 expression in transgenic brains revealed a more consistent expression in posterior medial-dorsal areas of the dorsal telencephalon compared with lateral and anterior areas (e.g. Fig. 1F,G and not shown). In line with this, the visual cortex generally appeared to be the most severely affected neocortical area (e.g. Fig. 3F). Although molecular marker analyses indicated a general deficiency in subsets of outer and deep layer pyramidal neurons in posterior areas, we did observe clusters of neurons expressing outer layer markers at lateral axial positions (Fig. 5N,P). This is consistent with a variable expressivity of the Zbtb20 transgene during neocortical neurogenesis. Alternatively, this heterogeneity in neocortical projection neuron development could potentially result from ectopic and heterochronical expression of exogenous Zbtb20 during early stages of corticoneurogenesis. The malformations of lamination result in behavioral abnormalities suggestive of impaired processing of visual and spatial memory traces in the cerebral cortex of adult Zbtb20 transgenic mice.

BTB-zinc finger factors can regulate key developmental processes in organisms as diverse as insects and mammals. In the fly nervous system, the BTB-zinc finger protein Chinmo was recently reported to specify temporal identity of neuroblast progeny (Doe, 2006; Zhu et al., 2006). In both mushroom body and projection neuron lineages, loss of Chinmo causes early-born neurons to adopt the fates of late-born neurons. In contrast, the temporal identity of mushroom body progeny was transformed toward an early fate by ectopic expression of Chinmo protein. The BTB-zinc finger factor Abrupt regulates the morphogenesis of class I dendritic aborization neurons, and ectopic expression of Abrupt in non-class I neurons altered the dendritic morphology of these cells (Li et al., 2004; Sugimura et al., 2004). Apart from Zbtb20, little is known about the role of BTB-zinc finger factors in neurogenesis of the mammalian brain. Outside the brain, the BTB-zinc finger factor Th-POK/cKrox functions as a molecular switch that turn immature thymocytes into CD4$^+$ helper T cells (He et al., 2005; Sun et al., 2005). Immature thymocytes develop into CD8$^+$ killer T cells in the absence of this BTB-zinc finger factor, whereas transgenic overexpression of the gene redirected major histocompatibility complex class I (CD8$^+$) cells to class II restricted CD4$^+$ helper T cells. Moreover, the Zbtb20-related Bcl-6 protein represses several genes that are necessary for terminal differentiation of B cells (Ahmad et al., 2003;

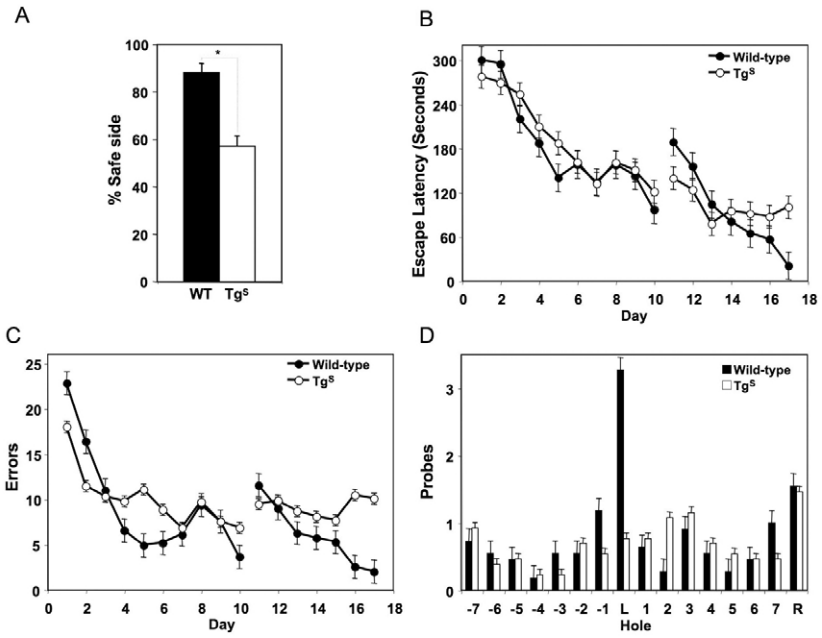

Fig. 6. Zbtb20^S transgenic mice display behavioral abnormalities. (**A**) Visual cliff measures of percentage of steps to safe side in age and sex-matched (females) wild-type (n=11) and Zbtb20^S (n=13) mice. *$P\leqslant0.001$. (**B-D**) Circular platform maze performed on the mice shown in (A). (B) Latency to enter the escape hole on each trial day. (C) Number of errors committed prior to locating the escape hole on each day of the trial. (D) Number of probes to the learning period escape hole (L) compared with approaches to all holes including the new reverse learning period escape hole (R) at the first trial day of the reverse learning period. All data are presented as means±s.e.m.

Kelly and Daniel, 2006). At the molecular level, BTB-zinc finger proteins have been proposed to be involved in chromatin remodeling, including transcriptional repression of downstream genes by recruitment of co-repressor-histone deacetylase complexes or polycomb group proteins (Ahmad et al., 2003; Barna et al., 2002; Gearhart et al., 2006; Kelly and Daniel, 2006).

The timely generation of CR neurons, deep and outer layer neurons and glial cells from cortical stem/progenitor cells appears to be regulated by a cell-intrinsic mechanism, whereby the latter cells become progressively restricted in developmental potential in vivo and ex vivo (Mizutani and Gaiano, 2006; Shen et al., 2006). As asymmetric divisions of cortical precursors result in cells with distinct fates, asymmetric distribution of cell-fate determinants is important for appropriate development of differentiated daughter cells and may also affect the developmental potential of the progenitor daughter cells. The telencephalic transcription factor Foxg1 is required to switch off CR neuronal fate in progenitors, whereas loss of Foxg1 in cortical progenitors results in untimely CR neurons production (Hanashima et al., 2004). The hippocampus-like transformation of the posterior retrosplenial cortex in Zbtb20 transgenic mice is remarkable, as pluripotent cortical precursors in this area normally generate subsets of neurons that settle in distinct layers. Our results are consistent with a model in which Zbtb20 functions as a molecular switch in a pathway that orchestrates invariant pyramidal neuron morphogenesis and

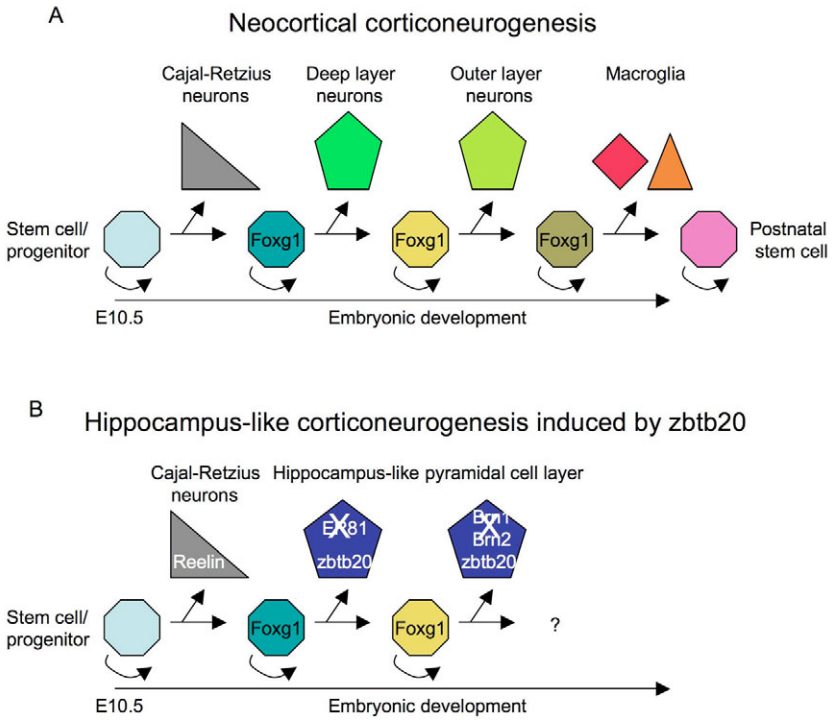

Fig. 7. Model. (**A**) Multipotent cortical progenitors harbor a cell-autonomous program in which, by asymmetric divisions, they become progressively restricted in developmental potential. At an early stage of corticoneurogenesis (around E10 in mice) they produce reelin-positive CR neurons followed by deep-layer and outer-layer pyramidal neurons and eventually macroglia [modified from Mizutani and Gaiano (Mizutani and Gaiano, 2006)]. The transcription factor Foxg1 appears to function as a constitutive active molecular switch required for early fate transitions in asymmetric proliferating precursors (i.e. by suppressing the production of reelin-positive CR neurons). (**B**) Ectopic expression of Zbtb20 in immature cortical pyramidal neurons leads to hippocampus-like neurogenesis of these cells apparently without affecting the early generation of CR neurons. The hippocampus-like transformations involved a deficiency in neurons expressing deep-layer (i.e. ER81) and outer-layer markers (i.e. Brn-1 and Brn-2) in Zbtb20 transgenic brains. The model suggests that Zbtb20 represses cell fate transitions in newborn pyramidal neurons and orchestrates the invariant morphogenesis of these neurons. The differentiation of macroglia from late precursors was not investigated in this work.

suppresses cell-fate transitions in newborn neurons (Fig. 7). The endogenous *Zbtb20* gene is expressed during the critical period of development of four homogenous populations of neurons in the mouse brain including pyramidal neurons in areas CA1 and CA3 and granule neurons in the dentate gyrus and cerebellum (Mitchelmore et al., 2002). It will be important to determine whether or not Zbtb20 is essential for invariant neurogenesis of these neurons. Moreover, as Zbtb20 is likely to be a high-level regulator of gene expression, identification of its target genes will be important to reveal factors that act downstream in the Zbtb20 pathway.

We acknowledge the expert technical assistance from Heidi Nielsen, Dr Thøger Rasmussen for help with setting up the circular platform maze, Dr Stefan Krauss for providing the D6-EGFP plasmid, Dr Franck Polleux for providing the pCIG2-EGFP plasmid, Dr Michael Wegner for providing the Oct-6 antibody and Dr Silvia Arber for providing the ER81 antibody. This work was supported by grants from the Lundbeck Foundation and the Danish Medical Research Council.

Supplementary material

Supplementary material for this article is available at http://dev.biologists.org/cgi/content/full/134/6/1133/DC1

References

Ahmad, K. F., Melnick, A., Lax, S., Bouchard, D., Liu, J., Kiang, C. L., Mayer, S., Takahashi, S., Licht, J. D. and Prive, G. G. (2003). Mechanism of SMRT corepressor recruitment by the BCL6 BTB domain. *Mol. Cell* **12**, 1551-1564.

Altman, J. and Bayer, S. A. (1990). Prolonged sojourn of developing pyramidal cells in the intermediate zone of the hippocampus and their settling in the stratum pyramidale. *J. Comp. Neurol.* **301**, 343-364.

Arber, S., Ladle, D. R., Lin, J. H., Frank, E. and Jessell, T. M. (2000). ETS gene Er81 controls the formation of functional connections between group Ia sensory afferents and motor neurons. *Cell* **101**, 485-498.

Barna, M., Merghoub, T., Costoya, J. A., Ruggero, D., Branford, M., Bergia, A., Samori, B. and Pandolfi, P. P. (2002). Plzf mediates transcriptional repression of HoxD gene expression through chromatin remodeling. *Dev. Cell* **3**, 499-510.

Corbo, J. C., Deuel, T. A., Long, J. M., LaPorte, P., Tsai, E., Wynshaw-Boris, A. and Walsh, C. A. (2002). Doublecortin is required in mice for lamination of the hippocampus but not the neocortex. *J. Neurosci.* **22**, 7548-7557.

D'Arcangelo, G., Nakajima, K., Miyata, T., Ogawa, M., Mikoshiba, K. and Curran, T. (1997). Reelin is a secreted glycoprotein recognized by the CR-50 monoclonal antibody. *J. Neurosci.* **17**, 23-31.

Doe, C. Q. (2006). Chinmo and neuroblast temporal identity. *Cell* **127**, 254-256.

Fishell, G. (1995). Striatal precursors adopt cortical identities in response to local cues. *Development* **121**, 803-812.

Fox, M. W. (1965). The visual cliff test for the study of visual depth perception in the mouse. *Anim. Behav.* **13**, 232-233.

Frantz, G. D., Bohner, A. P., Akers, R. M. and McConnell, S. K. (1994). Regulation of the POU domain gene SCIP during cerebral cortical development. *J. Neurosci.* **14**, 472-485.

Galceran, J., Miyashita-Lin, E. M., Devaney, E., Rubenstein, J. L. and Grosschedl, R. (2000). Hippocampus development and generation of dentate gyrus granule cells is regulated by LEF1. *Development* **127**, 469-482.

Gearhart, M. D., Corcoran, C. M., Wamstad, J. A. and Bardwell, V. J. (2006). Polycomb group and SCF ubiquitin ligases are found in a novel BCOR complex that is recruited to BCL6 targets. *Mol. Cell. Biol.* **26**, 6880-6889.

Hanashima, C., Li, S. C., Shen, L., Lai, E. and Fishell, G. (2004). Foxg1 suppresses early cortical cell fate. *Science* **303**, 56-59.

Hand, R., Bortone, D., Mattar, P., Nguyen, L., Heng, J. I., Guerrier, S., Boutt, E., Peters, E., Barnes, A. P., Parras, C. et al. (2005). Phosphorylation of Neurogenin2 specifies the migration properties and the dendritic morphology of pyramidal neurons in the neocortex. *Neuron* **48**, 45-62.

He, X., He, X., Dave, V. P., Zhang, Y., Hua, X., Nicolas, E., Xu, W., Roe, B. A. and Kappes, D. J. (2005). The zinc finger transcription factor Th-POK regulates CD4 versus CD8 T-cell lineage commitment. *Nature* **433**, 826-833.

Ishizuka, N. (2001). Laminar organization of the pyramidal cell layer of the subiculum in the rat. *J. Comp. Neurol.* **435**, 89-110.

Jensen, N. A., Rodriguez, M. L., Garvey, J. S., Miller, C. A. and Hood, L. (1993). Transgenic mouse model for neurocristopathy: Schwannomas and facial bone tumors. *Proc. Natl. Acad. Sci. USA* **90**, 3192-3196.

Johnston, D. and Amaral, D. G. (1998). Hippocampus. *The Synaptic Organization of the Brain*, 4th edn (ed. G. M. Shepherd), pp. 417-458. Oxford: Oxford University Press.

Kelly, K. F. and Daniel, J. M. (2006). POZ for effect–POZ-ZF transcription factors in cancer and development. *Trends Cell Biol.* **16**, 578-587.

Lee, S. M., Tole, S., Grove, E. and McMahon, A. P. (2000). A local Wnt-3a signal is required for development of the mammalian hippocampus. *Development* **127**, 457-467.

Li, W., Wang, F., Menut, L. and Gao, F. B. (2004). BTB/POZ-zinc finger protein abrupt suppresses dendritic branching in a neuronal subtype-specific and dosage-dependent manner. *Neuron* **43**, 823-834.

Machon, O., van den Bout, C. J., Backman, M., Rosok, O., Caubit, X., Fromm, S. H., Geronimo, B. and Krauss, S. (2002). Forebrain-specific promoter/enhancer D6 derived from the mouse Dach1 gene controls expression in neural stem cells. *Neuroscience* **112**, 951-966.

Machon, O., van den Bout, C. J., Backman, M., Kemler, R. and Krauss, S. (2003). Role of beta-catenin in the developing cortical and hippocampal neuroepithelium. *Neuroscience* **122**, 129-143.

McConnell, S. K. and Kaznowski, C. E. (1991). Cell cycle dependence of laminar determination in developing neocortex. *Science* **254**, 282-285.

McEvilly, R. J., de Diaz, M. O., Schonemann, M. D., Hooshmand, F. and Rosenfeld, M. G. (2002). Transcriptional regulation of cortical neuron migration by POU domain factors. *Science* **295**, 1528-1532.

Mitchelmore, C., Kjaerulff, K. M., Pedersen, H. C., Nielsen, J. V., Rasmussen, T. E., Fisker, M. F., Finsen, B., Pedersen, K. M. and Jensen, N. A. (2002). Characterization of two novel nuclear BTB/POZ domain zinc finger isoforms. Association with differentiation of hippocampal neurons, cerebellar granule cells, and macroglia. *J. Biol. Chem.* **277**, 7598-7609.

Miyata, T., Maeda, T. and Lee, J. E. (1999). NeuroD is required for differentiation of the granule cells in the cerebellum and hippocampus. *Genes Dev.* **13**, 1647-1652.

Mizutani, K. and Gaiano, N. (2006). Chalk one up for 'nature' during neocortical neurogenesis. *Nat. Neurosci.* **9**, 717-718.

Montenegro, M. A., Kinay, D., Cendes, F., Bernasconi, A., Bernasconi, N., Coan, A. C., Li, L. M., Guerreiro, M. M., Guerreiro, C. A., Lopes-Cendes, I. et al. (2006). Patterns of hippocampal abnormalities in malformations of cortical development. *J. Neurol. Neurosurg. Psychiatr.* **77**, 367-371.

Monuki, E. S. and Walsh, C. A. (2001). Mechanisms of cerebral cortical patterning in mice and humans. *Nat. Neurosci.* **4** Suppl. 1199-1206.

Nakahira, E. and Yuasa, S. (2005). Neuronal generation, migration, and differentiation in the mouse hippocampal primoridium as revealed by enhanced green fluorescent protein gene transfer by means of in utero electroporation. *J. Comp. Neurol.* **483**, 329-340.

Ohkubo, Y., Uchida, A. O., Shin, D., Partanen, J. and Vaccarino, F. M. (2004). Fibroblast growth factor receptor 1 is required for the proliferation of hippocampal progenitor cells and for hippocampal growth in mouse. *J. Neurosci.* **24**, 6057-6069.

Pompl, P. N., Mullan, M. J., Bjugstad, K. and Arendash, G. W. (1999). Adaptation of the circular platform spatial memory task for mice: use in detecting cognitive impairment in the APP(SW) transgenic mouse model for Alzheimer's disease. *J. Neurosci. Methods* **87**, 87-95.

Qian, X., Davis, A. A., Goderie, S. K. and Temple, S. (1997). FGF2 concentration regulates the generation of neurons and glia from multipotent cortical stem cells. *Neuron* **18**, 81-93.

Rakic, P. (2006). A century of progress in corticoneurogenesis: from silver impregnation to genetic engineering. *Cereb. Cortex* **16** Suppl. 1, i3-i17.

Shen, Q., Wang, Y., Dimos, J. T., Fasano, C. A., Phoenix, T. N., Lemischka, I. R., Ivanova, N. B., Stifani, S., Morrisey, E. E. and Temple, S. (2006). The timing of cortical neurogenesis is encoded within lineages of individual progenitor cells. *Nat. Neurosci.* **9**, 743-751.

Sock, E., Enderich, J., Rosenfeld, M. G. and Wegner, M. (1996). Identification of the nuclear localization signal of the POU domain protein Tst-1/Oct6. *J. Biol. Chem.* **271**, 17512-17518.

Sugimura, K., Satoh, D., Estes, P., Crews, S. and Uemura, T. (2004). Development of morphological diversity of dendrites in Drosophila by the BTB-zinc finger protein abrupt. *Neuron* **43**, 809-822.

Sun, G., Liu, X., Mercado, P., Jenkinson, S. R., Kypriotou, M., Feigenbaum, L., Galera, P. and Bosselut, R. (2005). The zinc finger protein cKrox directs CD4 lineage differentiation during intrathymic T cell positive selection. *Nat. Immunol.* **6**, 373-381.

Sur, M. and Rubenstein, J. L. (2005). Patterning and plasticity of the cerebral cortex. *Science* **310**, 805-810.

Tabata, H. and Nakajima, K. (2001). Efficient in utero gene transfer system to the developing mouse brain using electroporation: visualization of neuronal migration in the developing cortex. *Neuroscience* **103**, 865-872.

Tanaka, T., Koizumi, H. and Gleeson, J. G. (2006). The doublecortin and doublecortin-like kinase 1 genes cooperate in murine hippocampal development. *Cereb. Cortex* **16** Suppl. 1, i69-i73.

Tole, S., Goudreau, G., Assimacopoulos, S. and Grove, E. A. (2000). Emx2 is required for growth of the hippocampus but not for hippocampal field specification. *J. Neurosci.* **20**, 2618-2625.

Yoneshima, H., Yamasaki, S., Voelker, C. C., Molnar, Z., Christophe, E., Audinat, E., Takemoto, M., Nishiwaki, M., Tsuji, S., Fujita, I. et al. (2006). Er81 is expressed in a subpopulation of layer 5 neurons in rodent and primate neocortices. *Neuroscience* **137**, 401-412.

Zhao, Y., Sheng, H. Z., Amini, R., Grinberg, A., Lee, E., Huang, S., Taira, M. and Westphal, H. (1999). Control of hippocampal morphogenesis and neuronal differentiation by the LIM homeobox gene Lhx5. *Science* **284**, 1155-1158.

Zhu, S., Lin, S., Kao, C. F., Awasaki, T., Chiang, A. S. and Lee, T. (2006). Gradients of the Drosophila Chinmo BTB-zinc finger protein govern neuronal temporal identity. *Cell* **127**, 409-422.